Supplementary Figures

sNucDrop-Seq: Dissecting cell-type composition and neuronal activity state in mammalian brains by massively parallel single-nucleus RNA-Seq

Peng Hu[1,2,*], Emily Fabyanic[1,2,*], Zhaolan Zhou[1,2,#], and Hao Wu[1,2,#]

[1]Department of Genetics, [2]Epigenetics Institute, Perelman School of Medicine, Philadelphia PA 19104, USA

*These authors contributed equally to this work

#Correspondence to haowu2@upenn.edu (HW)

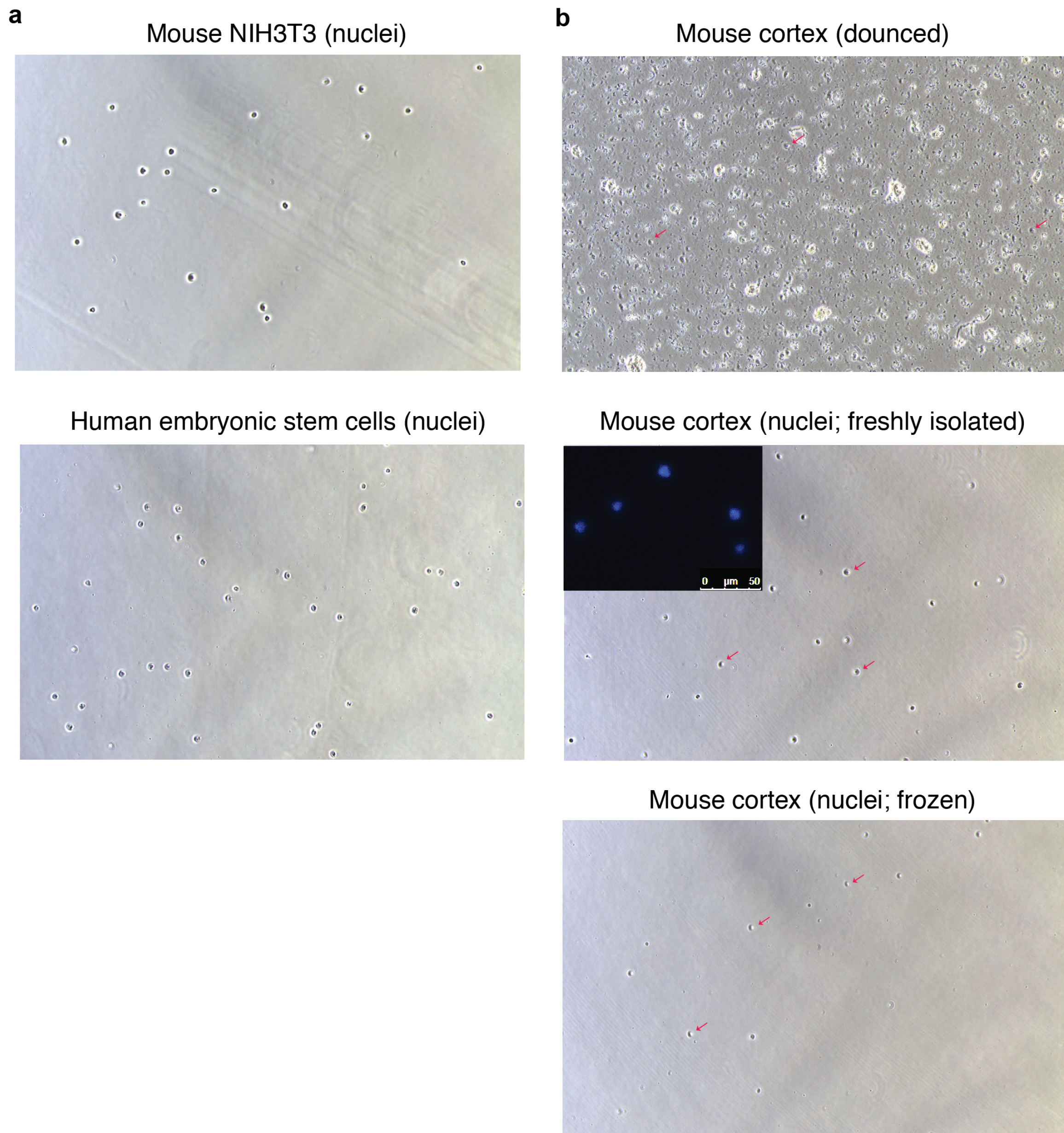

Supplementary Figure 1 | Quality control of nuclei isolation.

(a) After sucrose gradient centrifugation and filtering through cell mesh, mouse (top, NIH3T3) and human (bottom, embryonic stem cells (ESCs)) nuclei were visualized by phase-contrast microscopy (10x).

(b) After dounce homogenization, mouse cortical nuclei were visualized by phase-contrast microscopy (10x) before (top) or after (bottom) sucrose gradient centrifugation. Red arrows indicate nuclei before or after sucrose gradient

centrifugation. The inlet indicates fluorescent image of purified nuclei stained with DNA intercalating dye Hoechst 33342 (10 ng/μL). Scale bar, 50 μm.

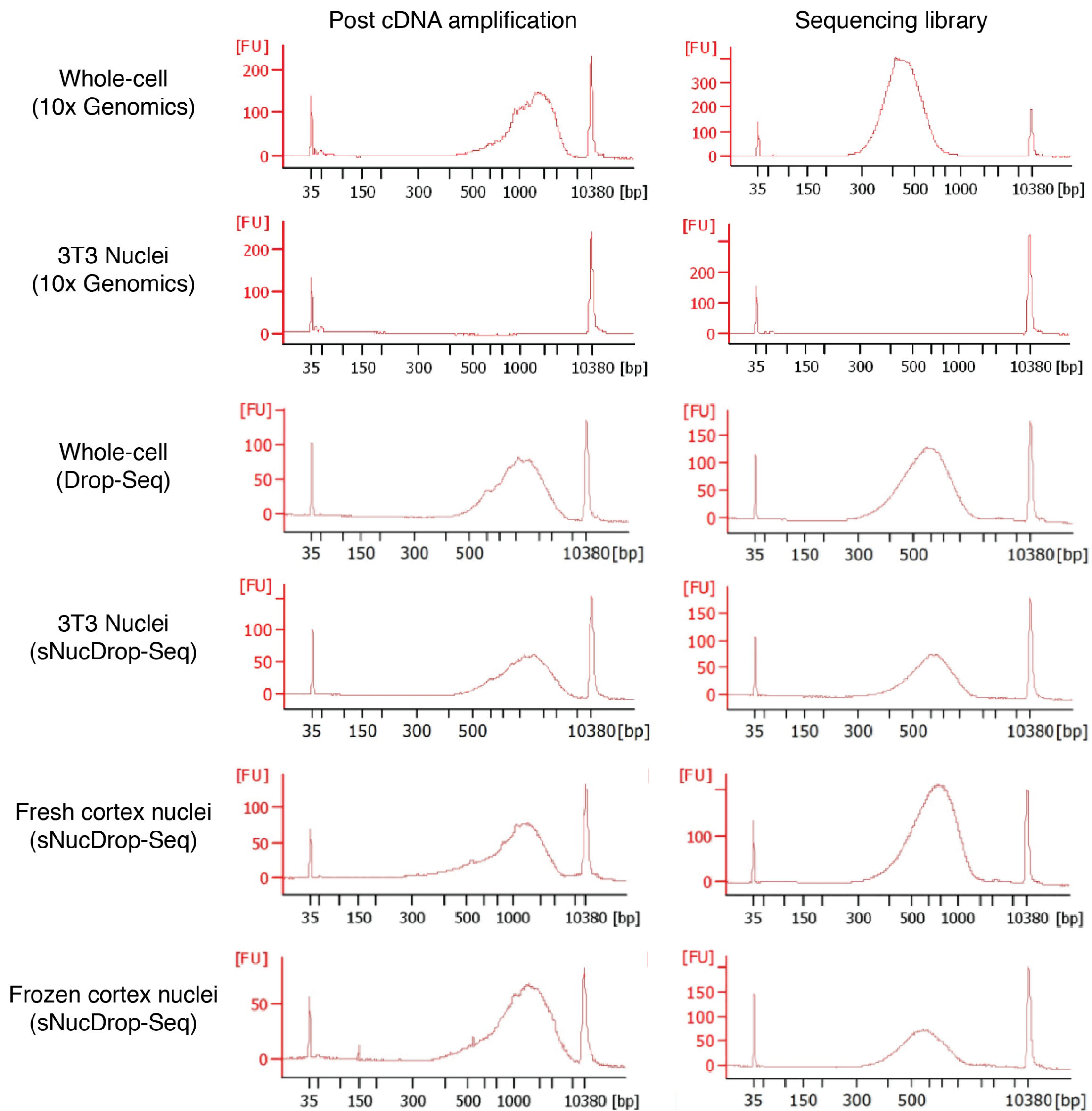

Supplementary Figure 2 | Testing different microfluidics platforms and library preparation workflows for single-nucleus RNA-Seq.

Bioanalzyer electropherogram of amplified cDNA (left) and final sequencing library (right) shown for samples prepared from whole-cell or nuclei by different platforms (10x Genomics platform or Drop-Seq/sNucDrop-Seq). FU, fluorescence units.

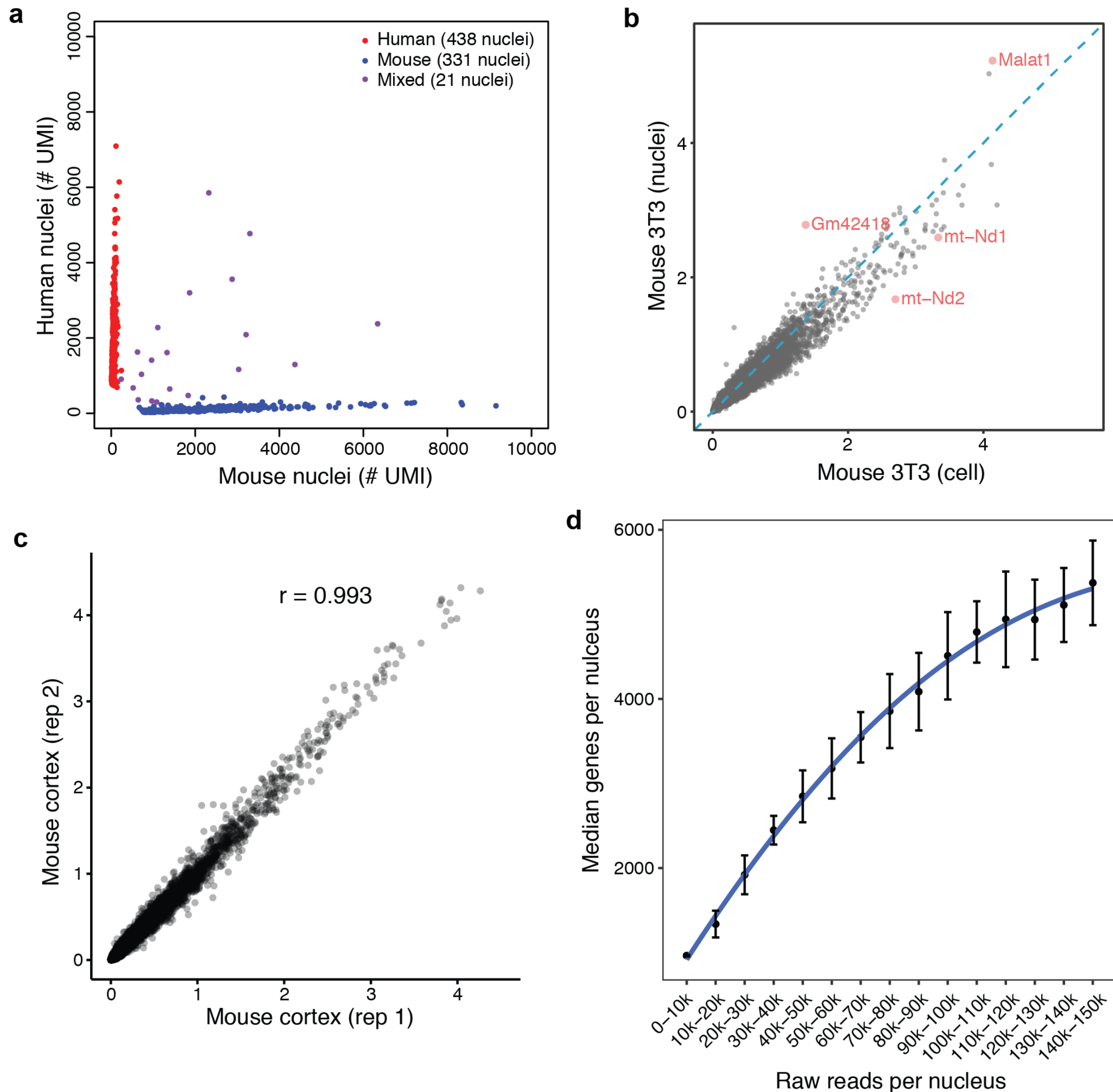

Supplementary Figure 3 | Specificity and performance of sNucDrop-Seq.

(**a**) Multi-species nuclei-mixing experiment measures sNucDrop-Seq specificity, by sequencing a mix of human (ESCs) and mouse (NIH3T3) nuclei. Scatter plot shows the number of transcripts (UMIs) associated with annotated human (y-axis) or mouse (x-axis) transcripts for each nucleus (dot). Nuclei with >80% human transcripts are labeled as human (red), and nuclei with >80% mouse transcripts are labeled as mouse (blue). Nuclei with a relatively high percentage of both human and mouse transcripts are labeled as mixed (purple). Of the 790 nuclei that passed quality filter (>800 UMIs), 21 (2.66%) had a mixed phenotype.

(**b**) Scatter plot comparing the average expression levels detected in single NIH3T3 nuclei (y-axis, by sNucDrop-Seq) and cells (x-axis, by Drop-Seq). Red dots mark representative genes preferentially enriched in either nuclei or cytoplasm (cell). For comparison, digital expression matrices of cell and nuclei were first combined, and UMI counts were then scaled by library size (total UMI counts per cell or nuclei), multiplied by 10,000 and natural log transformed. Only cells or nuclei that expressed >800 genes were retained for analysis. For each gene, the average normalized expression level were calculated as log (normalized UMI counts + 1).

(**c**) Scatter plot showing the high correlation of average expression levels [log (normalized UMI counts + 1)] between two biological replicates of sNucDrop-Seq analysis of mouse cortex.

(**d**) Median number of genes detected per nucleus at different raw reads per nucleus. Data from two independent experiments were included, mean±s.e.m.

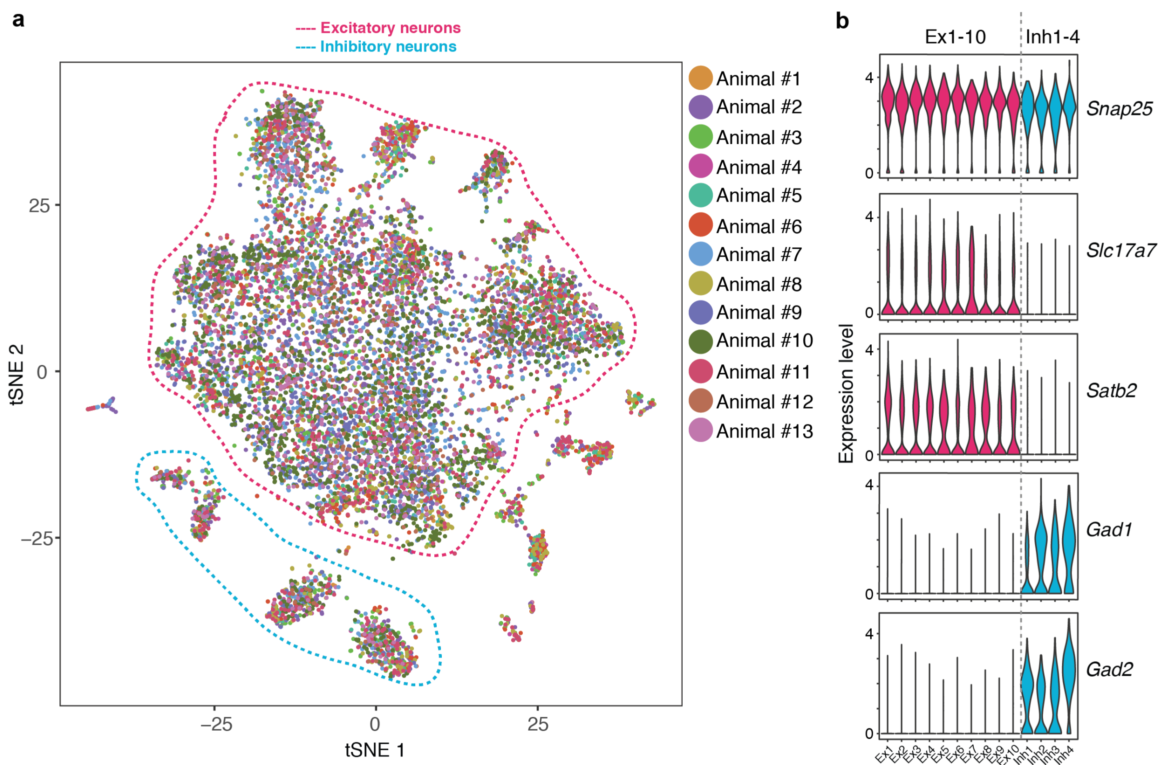

Supplementary Figure 4 | Cluster composition and neuronal marker gene expression.

(**a**) The tSNE plot (the same plot as in Fig. 1c) with all nuclei colored according to animal identity. Clusters corresponding to excitatory (red dashed line) and inhibitory (blue dashed line) neurons are grouped together.

(**b**) Violin plot illustrating the expression of pan-neuronal (*Snap25*), excitatory neuronal (*Slc17a7, Satb2*) and inhibitory neuronal (*Gad1, Gad2*) markers for excitatory (red, Ex1-10) and inhibitory (blue, Inh 1-4) neuronal clusters.

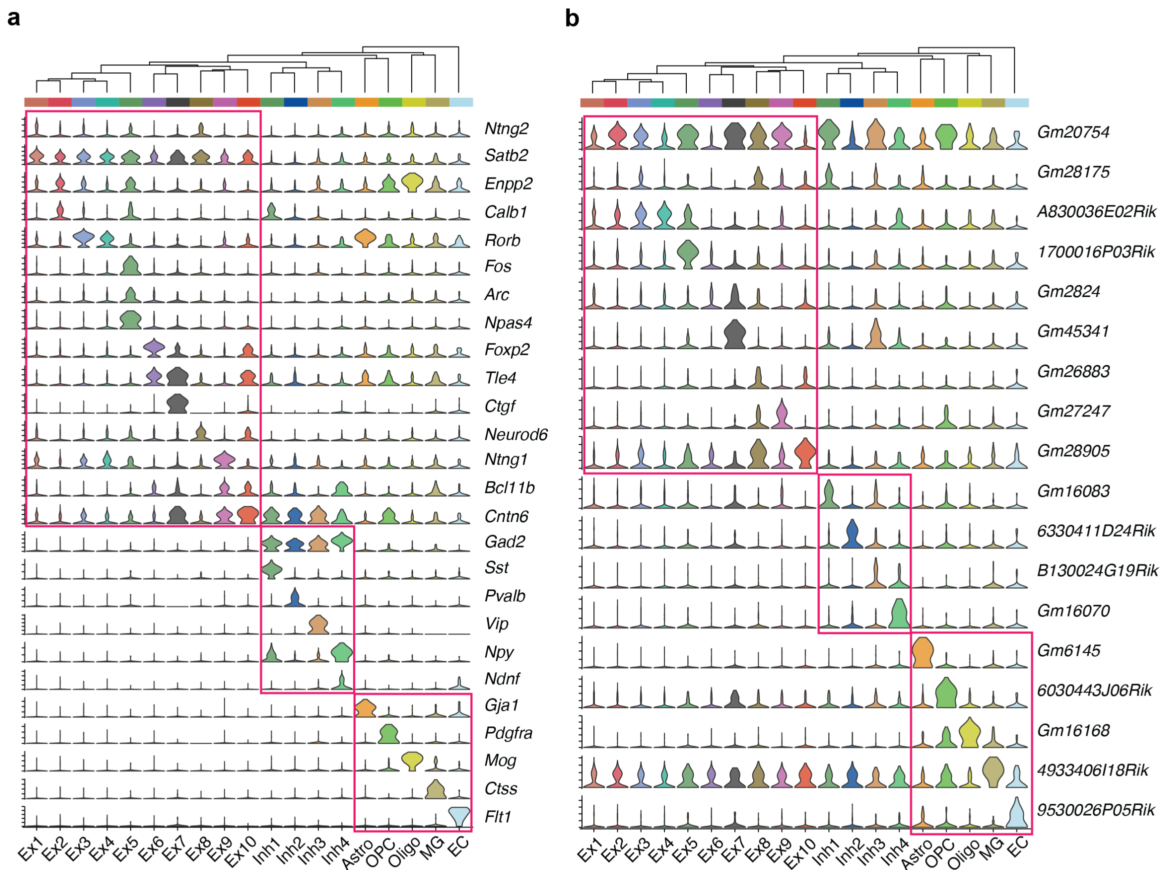

Supplementary Figure 5 | Protein-coding and noncoding marker gene expression for neuronal and non-neuronal cell clusters.

Violin plots illustrating select protein-coding (**a**) and non-coding (**b**) marker gene expression for excitatory neuronal (Ex1-10), inhibitory neuronal (Inh 1-4) and non-neuronal (Astro, OPC, Oligo, MG, EC) cell clusters.

a

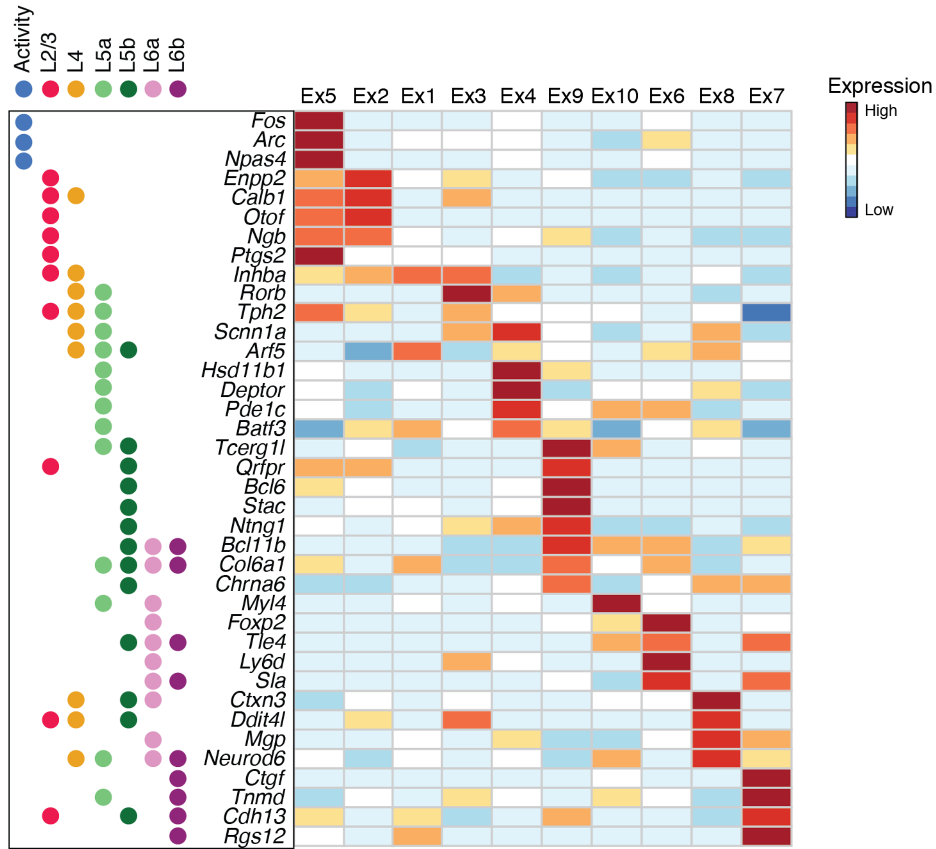

b

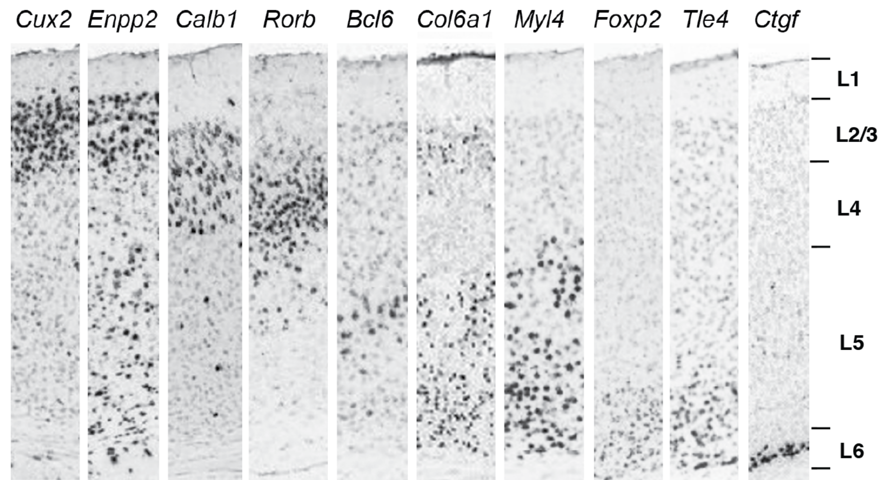

Supplementary Figure 6 | Cortical layer identity and activity-dependent transcriptional states of excitatory neurons.

(**a**) Heatmap showing layer-specific markers (L2/3/, L4, L5a/b, L6a/b) and neuronal activity-regulated gene expression in excitatory neuronal clusters (Ex 1-10 identified Fig. 1c).

(**b**) RNA in situ hybridization (ISH) showing layer-specific expression of selected markers in the mouse adult cortex (postnatal day 56, Allen Brain Atlas).

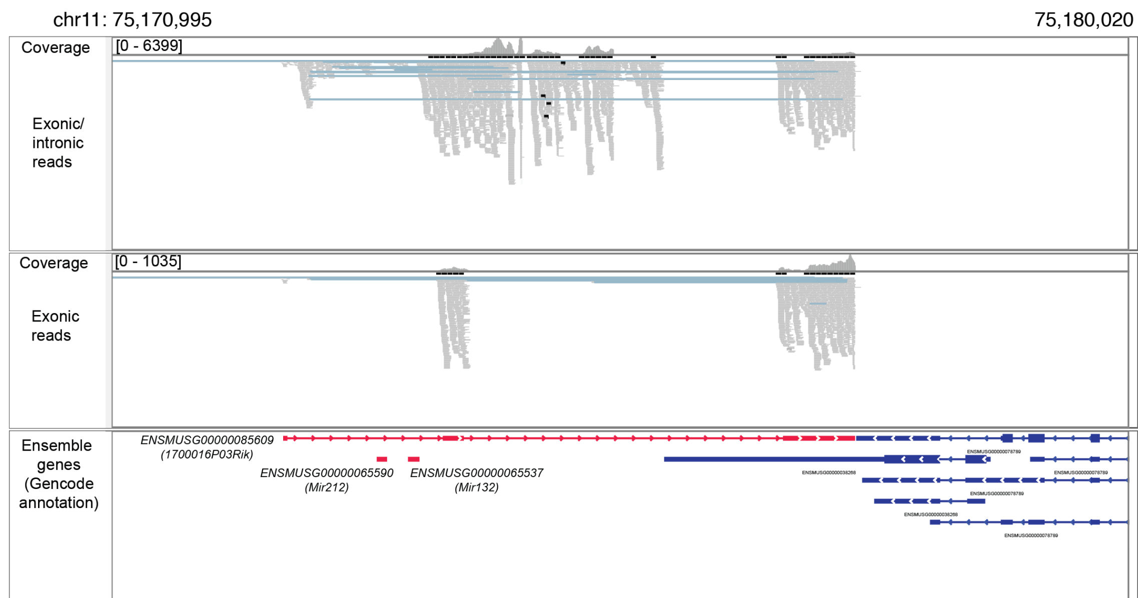

Supplementary Figure 7 | Distribution of exonic and intronic reads mapped to an activity-regulated non-coding transcript.

Genome browser view (build: mm10) of exonic and intronic reads (from sNucDrop-Seq of mouse cortex) mapped to *1700016P03Rik* (highlighted in red), a neuronal activity-induced non-coding transcript that encodes two microRNAs (Mir212 and Mir132).

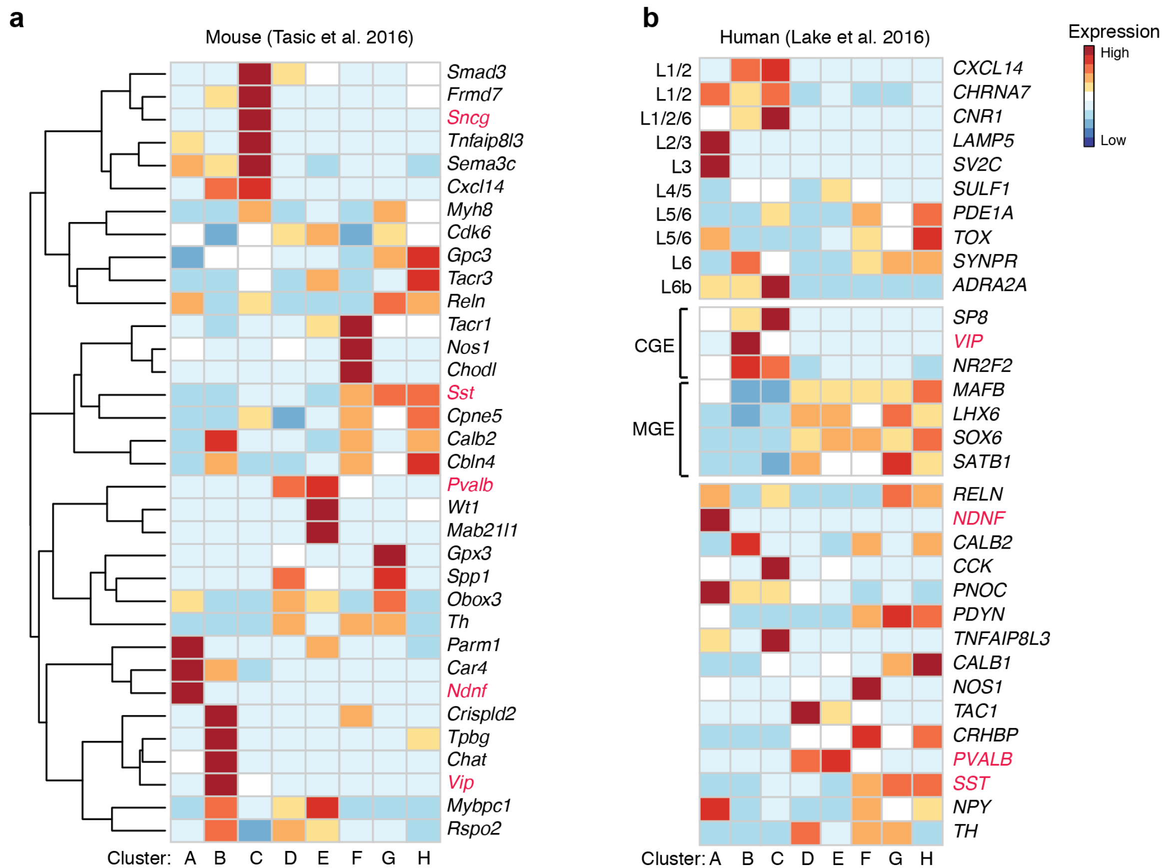

Supplementary Figure 8 | Marker gene expression for inhibitory neuronal subtypes. Heatmap illustrating select mouse (**a**) and human (**b**) marker gene expression for cortical inhibitory neuronal sub-populations (cluster A-H) identified in Fig. 2a. The mouse marker gene list is derived from Tasic et al. (2016) [1]. The human marker gene list is derived from Lake et al. (2016) [2]. Five mutually exclusive subtype-specific marker genes are highlighted in red. CGE, caudal ganglionic eminences; MGE, medial ganglionic eminences.

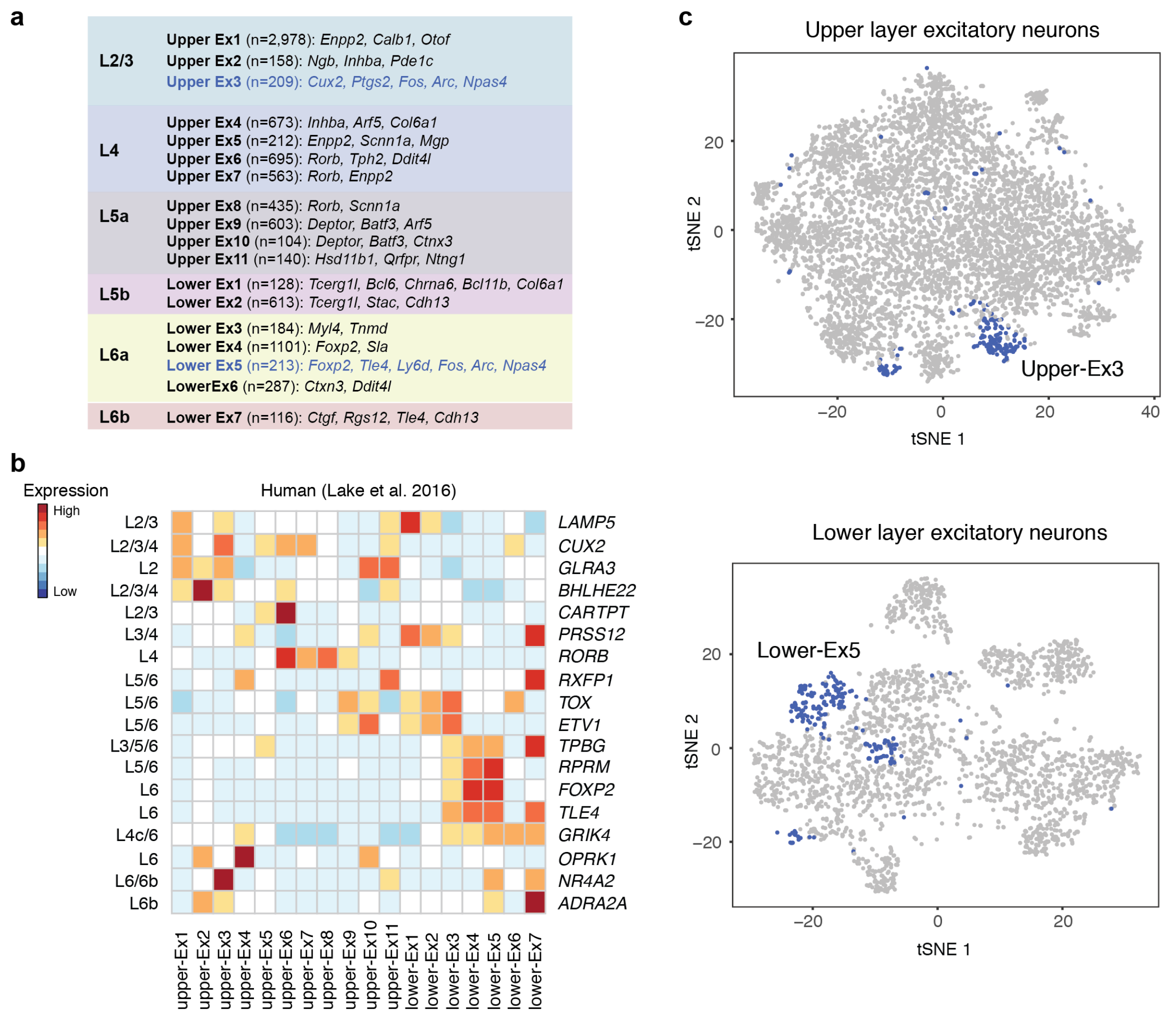

Supplementary Figure 9 | Cortical layer- and neuronal activity-dependent marker gene expression for excitatory neuronal subtypes.

(**a**) Summary of excitatory neuronal subtypes identified by sNucDrop-Seq. Glutamatergic neuronal subtypes are grouped according to cortical layer distribution. Also shown are number of nuclei per subtype and representative marker genes for each subtype.

(**b**) Heatmap showing select human marker gene expression for cortical excitatory neuronal sub-populations identified in Fig. 3a. The human marker gene list is derived from Lake et al. (2016) [2].

(**c**) Spectral tSNE plots (the same plots in Fig. 3a) highlighting activated excitatory neurons in upper (top, upper-Ex3) and lower (bottom, lower-Ex5) layer sub-clusters.

References

1. Tasic, B. et al. Adult mouse cortical cell taxonomy revealed by single cell transcriptomics. *Nat Neurosci* **19**, 335-346 (2016).
2. Lake, B.B. et al. Neuronal subtypes and diversity revealed by single-nucleus RNA sequencing of the human brain. *Science* **352**, 1586-1590 (2016).